T.1: Microfabrication using Indus-2 Soft and Deep X-ray lithography beamline

V. P. Dhamgaye[a] and G. S. Lodha[b]
Indus Synchrotron Utilization Division
[a]*vishal@rrcat.gov.in and* [b]*lodha@rrcat.gov.in*

Introduction

X-ray lithography is a 1X proximity shadow printing process for fabrication of high aspect ratio (HAR) structures where absorber pattern of an X-ray mask is recorded on X-ray sensitive photo resist using X-ray beam[1]. High intensity, low divergence X-rays from synchrotron radiation source offers a facility for the fabrication of high spatial resolution HAR structures. X-ray lithography is being used for the fabrication of variety of structures, such as compound refractive lens [2], submicron HAR structures [3], anti scatter grids [4], ultra thick and ultra high aspect ratio microstructures [5], etc. These devices are being used in multiple disciplines like optical, mechanical, electrical, biological, chemical domains.

Indus-2 is synchrotron radiation source operating at 2.5 GeV, 100mA and offers significant flux of X-ray energies upto 40keV. Several X-ray lithography beamlines are operational on synchrotron facilities [6, 7, 8, 9]. X-ray lithography beamline is installed on Indus-2 for undertaking microfabrication research activities. The beamline is designed to offer wide lithography window and it can be used for soft X-ray lithography (SXRL) for the fabrication higher spatial resolution structures and deep X-ray lithography (DXRL) for fabrication of deep structures. X-ray mask technology for fabrication of HAR structures is developed in-house. The soft and deep X-ray lithography (SDXRL) is in operation since April 2011 and open to user to undertake the microfabrication research.

X-ray lithography was first carried out at IBM by Spiller et al in 1975 [10], when they fabricated the metal structure of gold by electro deposition in 20 µm thick PMMA mold. The X-ray microfabrication process was deployed by Ehrfeld et al at the Karlsruhe (Kernforschungszentrum Karlsruhe) in 1982 for fabrication of micron size nozzles for Uranium-235 enrichment [11]. They used 2.5GeV synchrotron radiation source for exposure of PMMA resist. After this, many synchrotron radiation sources have adapted the beamlines for undertaking the microfabrication activities. In 1990s, lots of works were carried out for establishing X-ray lithography as technique for replacing the UV lithography for ICs fabrication. However, X-ray lithography was unable to keep the pace against the improvement (resolution enhanced techniques) in optical lithography and hence failed in its industrial use for ICs fabrication. However, X-ray lithography is still in use in various synchrotron laboratories for fabrication of 3D high aspect ratio microstructures at R&D level.

Synchrotron radiation based X-ray lithography

X-rays obtained from synchrotron radiation sources have higher intensity and wider energy range than the X-ray obtained from plasma source or Coolidge tube X-ray sources. Synchrotron radiation has low divergence and high brightness thereby allowing shorter exposure times. Bending magnet based synchrotron radiation sources offers wider horizontal beam but reduced Gaussian beam size in vertical direction due to natural emission cone at ultra relativistic electron energy. To enlarge the beam in vertical direction for homogenous exposure on substrate, the substrate is moved in vertical direction in stationary path of the beam with the help of precision scanner. The substrate is scanned in the beam repeatedly until the desired dose on the substrate is obtained.

X-ray lithography is classified in the two categories depending upon the critical dimension and aspect ratio desired. The pattern of X-ray mask is transferred on X-ray sensitive photo resists using appropriate X-ray energy range producing variable depth and minimum feature sizes. X-ray energies from 1-2 keV are used to obtain the highest critical dimension (<100 nm) but lower depth, known as SXRL. On increasing X-ray energies, higher depth can be achieved using DXRL. X-ray energies (4-20 keV) are used to obtain a depth of 1500 micron and depth of 8-10 mm is obtained using X-ray energies upto 40keV.

X-ray LIGA

X-ray LIGA is German acronym for X-ray Lithography, Galvanoformung (electrodeposition) and Abformung (moulding) processes for fabrication of 3D HAR microstructures in polymers, metals and ceramics. Elemental steps involved in X-ray LIGA technique is shown in Figure T.1.1. From top, in the first step the latent image of X-ray mask is recorded on the photoresist (polymer). It is then developed in appropriate etching solution (step 2). The structure formed in polymer is then used as parent mold for electrodeposition of metal materials shown in step 3. Further polymer is removed and metal mold is achieved. Now this structure (step 4) can act as master mold for mass fabrication of polymer structure (step 5). The metal master mold can be used for ceramic filling at elevated temperature.

Thus in X-ray LIGA process, structures in polymers, metals and ceramics can be fabricated.

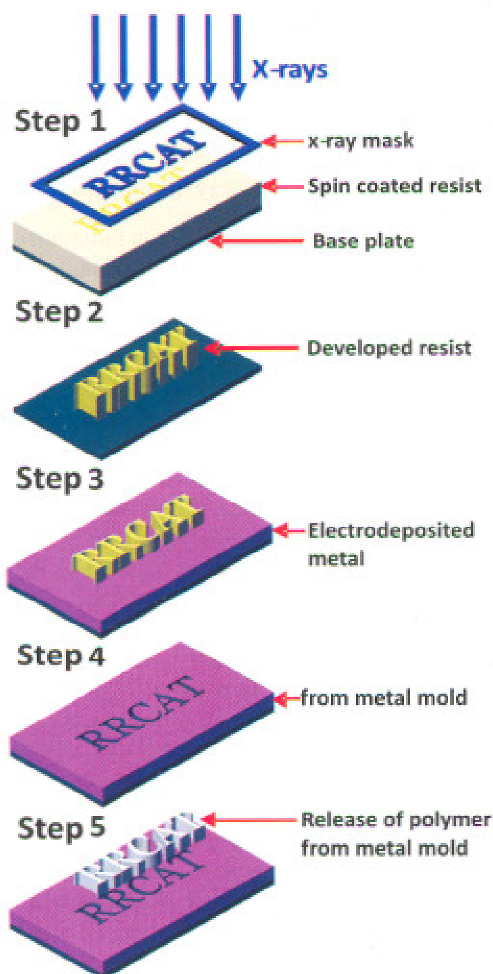

Figure T.1.1: Elemental steps involved in X-ray LIGA.

X-ray Resist

Poly(methylmethaacrylate), commercially known as PMMA is best resist in use due to its high resolution. However, it is less sensitive to X-rays and hence the exposure time is higher for obtaining deeper structures. Selection of energy deposition in PMMA should be judiciously chosen otherwise cracks and thermoelstatic deformation of resist occurs. In case of PMMA the exposure dose contrast of 5 is maintained between the top and bottom dose. This type of dose contrast is not required in SU-8 resist which is chemically amplified resist. SU-8 is a negative photoresist and has sensitivity 100 times greater than PMMA but has lower resolution in comparison to PMMA.

Beamline Description

Many groups around the world are operating the X-ray lithography facility on synchrotron storage rings. Most of them are for DXRL and some of them are for SXRL installed on dedicated storage rings. A beamline dedicated for soft and deep X-ray lithography is designed, built and commissioned on Indus-2 for research on (i) HAR, three-dimensional micro structures using hard X-rays and (ii) high spatial resolution (<100nm) structures using soft X-rays. The optical design of X-ray lithography beamline is described earlier [12]. Figure T.1.2 shows the optical design of the SDXRL beamline. Figure T.1.3 shows the mechanical layout of the installed SDXRL beamline. The beamline consist of two mirror system, slits, filters, Be window assemblies and X-ray scanner. With the help of two mirror system and absorption edge filters, the X-ray energy can be tuned between 1.5 keV and 20 keV. Beamline is designed for 1.5 keV where highest spatial resolution can be achieved due to reduced photoelectron blur. Beamline accepts 4σ vertical beam at 1.5 keV and offers penumbral blur of 0.56 mrad. The other geometrical blur is introduced by horizontal divergence of the beam, also known as runout error. For the designed energy and X-ray mirror(s) parameters, runout error is fixed to 2.5 mrad. Using the torroidal mirror and plane mirror, beamline offers the high flux and a homogeneous intensity profile (± 3%) in horizontal plane. Penumbral blur and runout error are optimized to 5.6 nm and 25 nm respectively for achieving minimum feature size of few tens of nanometers. The salient features of the beamline are given in Table T.1.1.

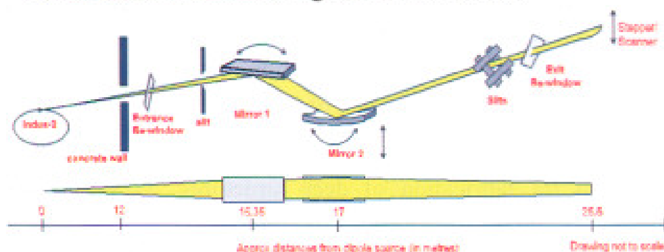

Figure T.1.2: Optical design layout of SDXRL beamline.

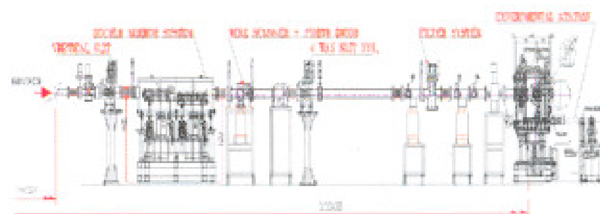

Figure T.1.3: Mechanical design of SDXRL beamline

The selection of various energy domains is achieved with combinations of filters and two mirrors. The beamline design allows continuous change of spectral range of interest [13]. Depending upon the depth of the structures required in

photo resist the beamline can be operated in high energy, low energy and high flux or edge absorber modified flux (power) modes.

Table T.1.1: Salient features of the beamline

Energy range	1.5 keV - 20 keV
Reflecting mirrors	Two mirrors (1 plane @ 16.2m and 1 torroidal @ 17m) Pt coated Si-substrate with side-cooling arrangement
Mirror sizes	100 x 650 mm^2
Beamline acceptance	Horizontal 5 mrad and Vertical 0.83 mrad 4σ (@1.5 keV)
Beam size at sample	~80 (Horizontal) x 10 (Vertical) mm^2
Angular Range	0.15 - 2.0 degrees
Filters	Be, C, Al

1. Two mirror mode of operation : Energy between 1.5 - 20 keV is tuned. Beam size is variable between 2mm (V) x 55mm (H) to 10 mm (V) x 90 mm (H) at the experimental station (depending on the energy band required during exposure)

2. Single mirror mode of operation : High energy and high flux, continuous energy spectrum from 5-20keV. Beam sizes is 10 mm (V) x 100 mm (H) at the experimental station

3. White beam (No optics) mode of operation : High energy upto 40 keV is available to create high depths in photoresist. Beam size at experimental station is 18 mm (V) x 100 mm (H).

Two mirror system

The heart of the beamline is a two mirror system where first mirror (M1) is installed at 16.2m and second mirror (M2) is installed at 17 m from the source point. Figure T.1.4 shows the installed view of two mirror system in the optics hutch of the beamline. M1 is a plane mirror and used as cuttoff reflector and absorb the radiation heat load. M2 is a torroidal mirror (with radii 420 m in meridional and 0.55m in sagittal direction) which focuses the beam in vertical direction (focusing distance 9.5m) and collimates the beam in horizontal direction (focusing distance 22m). Mirrors are coated with Pt layer with surface roughness of 5 Å and slope errors is ~5 μrad in meridional direction. Both mirrors are mounted on three point mirror manipulator mechanism which sets mirrors at grazing incidence angular range of 0-2° with an accuracy of ~5 μrad. The precision movement of mirrors in pitch and roll direction and effect on each other (pitch on roll and vice-versa) are measured using a laser interferometer. The measured accuracy of mirror positioning in pitch direction is ~ 5 μrad. The effect of roll on pitch and vice versa is also measured and found to be less than ~ 25 μrad.

Extensive ray tracing calculations are performed for the beamline design using simulation codes, RAY and SHADOW, ShadowVUI. All the factors which affect the high performance of the beamline like, figure errors, thermal slope errors and misalignment errors of the optical elements, are taken into the simulation and optimized the beamline design. Figure T.1.5 shows the point diagram of the SR beam at experimental station at designed energy. The size of the beam is 2 mm vertical and 55 mm horizontal, with horizontal intensity uniformity below ~ 3%. However, we reduce the height of the beam by using the slit apertures.

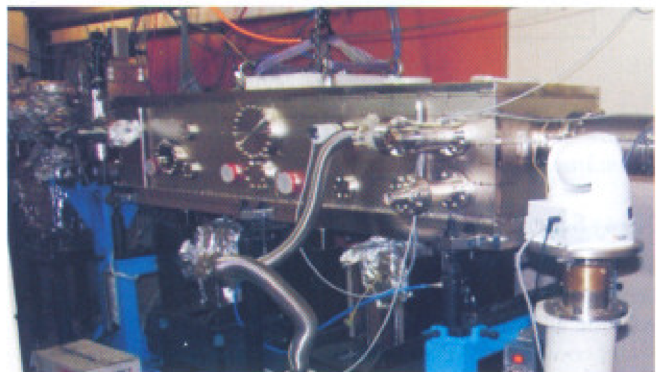

Figure T.1.4 : Installed view of two mirror system on SDXRL beamline optics hutch.

For exposing photo-resist at mask-wafer stage a wide beam with high spectral power is required. Figure T.1.6 gives the energy-power spectra for various mirror settings and thickness of Be-window.

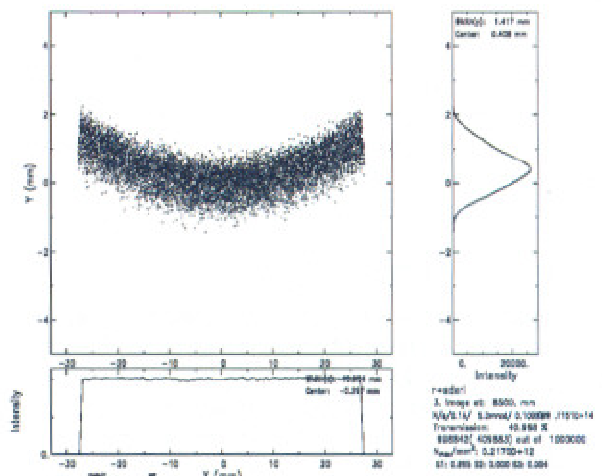

Figure T.1.5: Point diagram of SR beam at experimental station at 1.5 keV mirror settings.

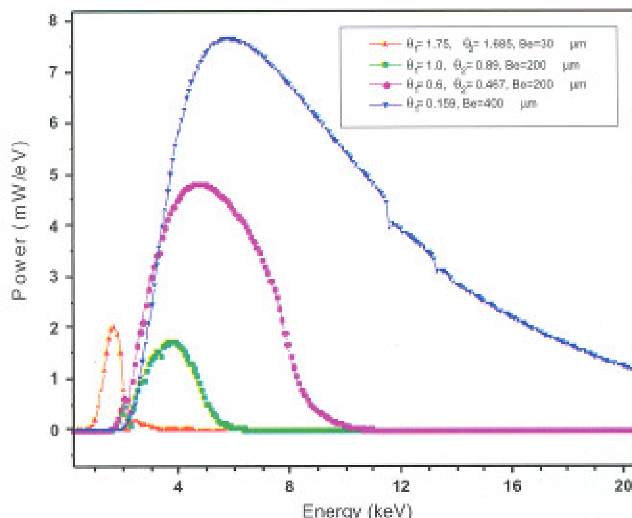

Figure T.1.6: Energy-Power spectrum offered by SDXRL beamline.

X-ray Scanner

Custom designed X-ray scanner system is installed in the experimental hutch. It consists of vertical scanning stage, rotation and tilt module, water cooled mask-wafer stage and water cooled apertures. The goniometer with rotation and tilt stages are mounted on vertical scanning stage supported by two linear guides and actuated by two stepping motors in synchronized motion. The vertical scanning stage can be moved for scanning range ± 90 mm with variable speed of 1-30mm/s. The variable scanning speeds helps to reduce the thermal load on photo resist and in turn controls its degradation. The X-ray mask and substrate of size 100 x 100 mm^2 can be mounted on X-ray mask wafer stage which can be rotated, tilted and scanned to fabricate three dimensional microstructures. The salient features of the X-ray scanner are given in table T.1.2. Figure T.1.7 shows the mask wafer stage assembly inside X-ray scanner with X-ray mask and PMMA resist in mounted condition. The scanner can be operated in vacuum or helium environment. X-ray Offline alignment stage is fabricated to align X-ray mask and photo resist with an accuracy of ~5 μm for multiple exposures.

X-ray mask development program

Typical X-ray mask consist of a supporting membrane and X-ray absorbing layer. Membrane is generally low atomic number materials and high Z materials are used to define the absorber pattern. SXRL and DXRL require different types of X-ray mask. In both the techniques, the mask membrane materials and the thickness of absorber layer may be different. It should be chosen to obtain the higher contrast between exposed and unexposed region at photoresist. For SXRL, the thickness of the absorbing layer is ~ 0.2-3 μm and for DXRL process the required thickness of absorbing layer is 10-30 μm. The structures obtained in the resist depend on the quality of produced X-ray mask. X-ray masks are produced using electron beam lithography and/or UV lithography. The X-ray mask required for DXRL process which is produced from electron beam lithography system requires two X-ray masks, first is intermediate X-ray mask where the absorber thickness is smaller and another is working X-ray mask produced using X-ray beamline. X-ray mask produced using UV lithography can be obtained to higher absorber thickness in single step. However, the quality of the electron beam produced X-ray mask is much better than the X-ray mask produced using UV lithography system.

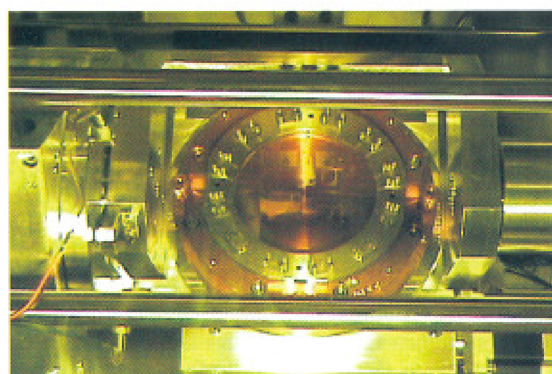

Figure T.1.7 : Inside view of X-ray scanner system where X-ray mask and resist are mounted for their X-ray exposures

Table T.1.2: Salient features of the X-ray scanner

Feature	Specification
Exposure window	± 90 mm (V), ± 40 mm (H)
Exposure Environment	Vacuum, He-gas, Air(inside chamber)
Mask-Substrate Size	Circular ϕ 100 mm and Square 100mm x 100mm
Photo resist thickness	1-5000 μm
Mask-Resist tilt and rotation	tilt 0-90° and rotation ± 180°
Gap between mask and resist	0-100 μm
Offline alignment stage	
For multiple exposure, to create 3 dimensional complex micro-structures, alignment accuracy between mask and photo resist is ~5 μm	

We have initiated the development of variety of X-ray masks based on their requirement in the application (device) specific and X-ray exposure energy range. Two types of X-ray masks are developed, one is low cost X-ray mask which is fabricated

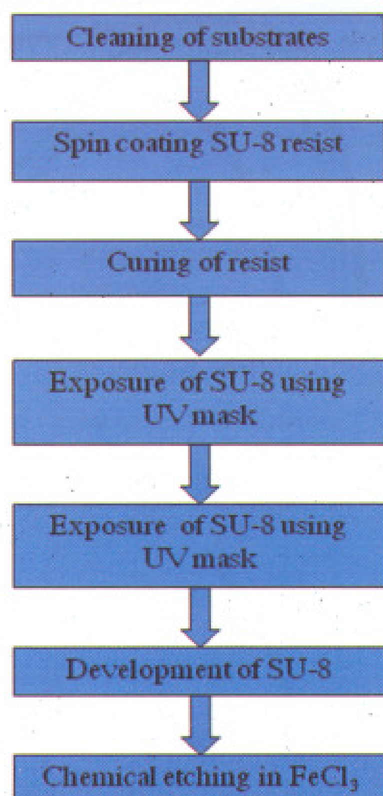

Figure T.1.8: Processing steps involved for fabrication of SS and Cu foil X-ray masks

using conventional method of photo chemical machining in stainless steel and copper foils and second type of X-ray mask fabricated with polymer membrane based gold absorbing layer using UV lithography process.

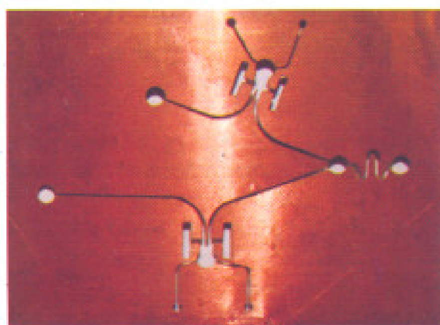

Figure T.1.9: Low cost X-ray mask fabricated in 100 m thick Cu foil.

Stainless steel and Copper foils, 100 µm thick are used to fabricate low cost X-ray mask. Required patterned is transferred on the resist coated on these foils using UV lithography. Subsequently, the developed structure of resist is etched out using ferric chloride solution. The processing steps involved in the fabrication of metal foil based X-ray mask is shown in figure T.1.8. Minimum feature size obtained in this type of X-ray mask is limited to the thickness of the foils and hence these X-ray masks are used for the patterns with feature sizes more than 100 µm. These masks are used for fabrication of microfluidic channels, lab on chip etc. Figure T.1.9 shows the X-ray mask fabricated for integrated lab on chip device in copper foil. X-ray mask with fine features with sharp edge profiles are obtained on thin membrane (polyimide/SU-8) based X-ray mask using UV lithography and gold electrodeposition techniques. The processes involved in the X-ray mask fabrication of this type of

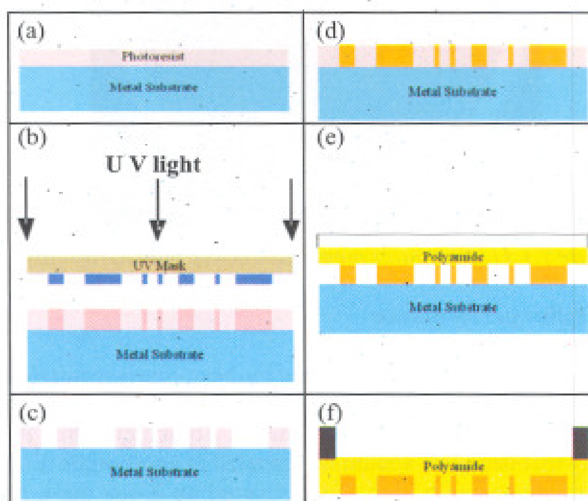

Figure T.1.10: Polyimide mask fabrication process: (a) 300 µm-thick metal substrate (brass wafer) was spin coated with photo reist S1813, (b) Exposure of S1813 using UV source (c) the exposed resist is developed and cavities are seen (d) S1813 mold was electroplated with gold (e) S1813 is removed and polyimide spin coated on gold electrodeposited brass wafer. (f) stainless steel ring (black) is fixed from polyimide side and finally brass substrate is etched.

mask is described in figure T.1.10. Initially, metal substrates are coated with UV resist, S1813. UV mask containing the patterns required in X-ray mask is exposed on S1813 using UV source (350-400 nm). Substrates are then developed in MF319 developer solution and mold is obtained in S1813, which is then used for electrodeposition of gold. Commercially available non cyanide gold plating solution is used for electro deposition. S1813 is removed using acetone by dipping. Polyimide solution is spin coated on the gold absorbing material and then cured at higher temperature to obtained 40 µm thickness. Lastly, stainless steel annular ring is fixed on the polimide and brass wafer is etched out in nitric acid. The final fabricated X-ray mask is shown in Figure T.1.11. Similarly, SU-8 membrane based X-ray masks are also fabricated using similar technique described above and replacing the polyimide with SU-8 resist. Membrane based

X-ray mask can also be used for multi-level X-ray LIGA process using multi exposure techniques. For the fabrication of ultra high resolution masks, electron beam lithography and deep reactive ion etching systems are being commissioned.

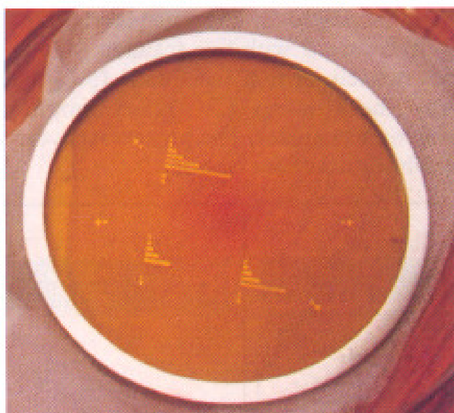

Figure T.1.11: Polyimide membrane based gold X-ray mask

Beamline performance

The high performance of the beamline is required for efficient fabrication of deep and ultra deep structures in PMMA/SU-8 X-ray sensitive resists. To achieve this, it is likely that beamline should be operated in appropriate X-ray energy ranges with high flux delivered on X-ray mask and substrates. The highest power is available in the beamline when it is operated in single mirror mode. In two mirror system configuration, highest power is available for grazing incidence angles ~ 0.2°. It is difficult to set both the mirrors smaller than this angle due the proximity of both mirror optical surface. Yet mirrors can be set for grazing incidence angles anywhere between $0.01\text{-}2.0^{\circ}$ independently. In a typical beamline operating condition when both the mirrors are set at 0.6°, we obtain the pink energy spectrum between 2-10keV. Figure T.1.12 shows the transmission characteristics of individual optical elements used in the beamline, X-ray mask and PMMA with 500 µm thickness. In this case, power incident on the X-ray mask (after two mirrors) is ~ 8.7 W (blue curve) and total incident power on the beamline is 49 W (black curve). In house developed, wire scanner is used to characterize the beam profile. Thin wire of W/Au of 60 µm in diameter is used to quantify the beam profile obtained downstream to the two mirror system. Figure T.1.13 shows the beam profile obtained after M2 at 18 m from the source point. At experimental station which is at distance of 25.5 from source point, the beam sizes for this typical operation condition are 10mm (V) and 80mm (H). For X-ray exposure of the X-ray mask and resist of 100mm diameter, beam is enlarged in vertical direction using X-ray scanner.

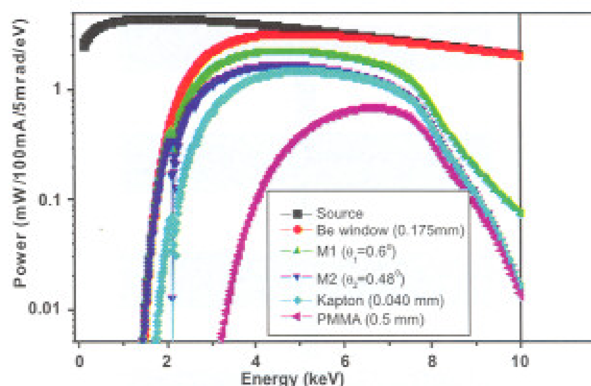

Figure T.1.12: Transmission characteristics (energy power) of a SDXRL beamline for typical operation condition.

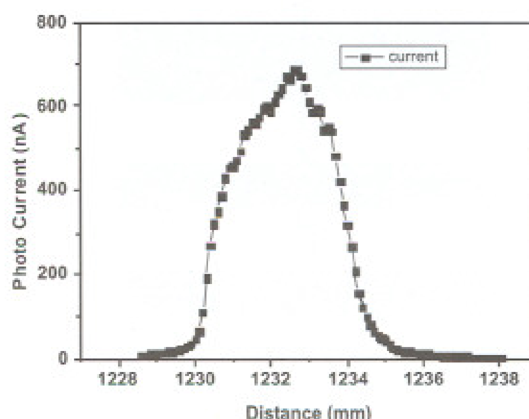

Figure T.1.13: Wire scan obtained at 18m from source when mirrors are set for 2-10keV spectrum.

Recent research activities

X-ray lithography beamline is used for development of various HAR microstructures in PMMA/SU-8. With present capabilities of this beamline, it is possible to cater both in house and outside users for microfabrication activities. In X-ray optics section, our goal is to develop reflective, refractive and diffractive X-ray optics for synchrotron beamline applications.

Understanding the interaction of X-rays with X-ray sensitive photo resist, PMMA and its development in developer solution is critical in order to obtain the high quality structure with reasonably good surface roughness. Recently, we have exposed the PMMA with various doses and studied the behavior of PMMA microstructures in GG developer under various conditions [15]. The GG developer is maintained at room temperature, high temperature and finally at agitated (ultrasonication) conditions at room temperature

for developing PMMA. The PMMA is exposed for radiation dose of 62167 mAsec/cm and dissolution rates of the PMMA resist in three different condition is shown in figure T.1.14. It shows that in case of ultrasonic agitation, higher depths are obtained in comparison to room and high temperature development condition. It is also observed that integrity of the structures are maintained in all conditions.

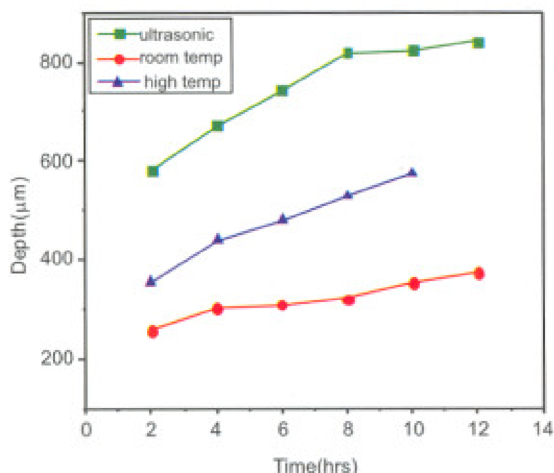

Figure T.1.14: Behavior of PMMA in GG Developer in three different conditions, room temperature, high temperature and ultrasonic agitation.

Compound refractive lenses (CRL) with a focal length of 1-2 m are a new tool for focusing hard X-rays to a spot size in the μm-nm range. They have been used for microdiffraction, microfluroscnence and coherent X-ray imaging. CRL may be focusing in one dimension and two dimensions depending upon their design. The focal length for CRL is given by:

$$f = \frac{R}{2N\delta}$$

where, f is focal length, R is radius of lens at the apex, N is number of lens and δ is index for refraction. The value of δ for PMMA is in the range of 10^{-6} for X-ray energy 8-12 keV. For single lens (N=1) and R = 100 μm, the calculated focal length will be ~ 50 m. In order to reduce the focal length, more number of lenses should be stacked in straight line. Parabolic profile CRLs are designed for focusing 8-12 keV X-rays and fabricated in PMMA is shown in Figure T.1.15. The fabricated CRLs has radius 100 μm at the apex, geometrical aperture of 400 μm and N= 1-50 number CRLs on the single chip. Recently one of the fabricated CRLs (N=50) is tested on synchrotron and 2 μm beam spot is obtained against the calculated 1 μm beam size. Various types of CRLs (parabolic and elliptical profile) are being fabricated and their investigations shall be carried out.

Figure T.1.15: Compound refractive lens fabricated in PMMA.

X-ray lithography can be extended to fabrication of 3D HAR structures using innovative exposure techniques. X-ray mask and resist can be moved relative to each other with various speeds in order to obtain the spherical, parabolic and hyperbolic structures. It is also possible to rotate and tilt the X-ray mask and resist together to obtain the tilted structures. Three dimensional tapered structure is fabricated in PMMA is shown in Figure T.1.16. In this case, two X-ray exposures are carried out, first exposure is with the help of X-ray mask. In second exposure, X-ray mask is removed and only bare PMMA resist is exposed to X-ray beam. It is further developed in GG developer for obtaining the profile. The top diameter of tapered curved neck holes is 200μm and bottom diameter is 100 μm.

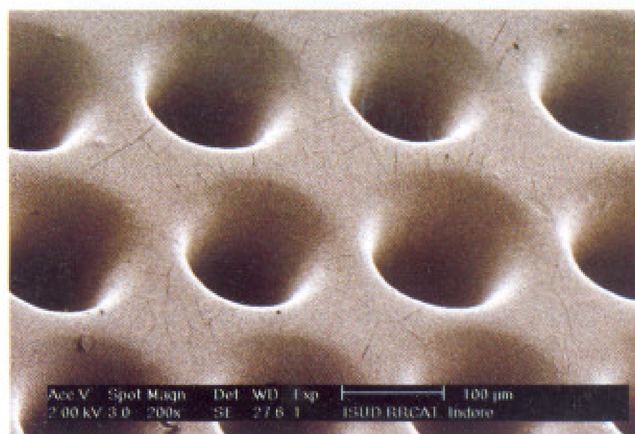

Figure T.1.16: Curved neck, tapered holes fabricated in PMMA using innovative exposure techniques.

Few simple devices in microfluidic are also demonstrated using this facility. A micro fluidic device may consists of micro channels, micromixers, micro valves,

micropumps, reaction chambers which are fabricated on the same chip for multifunctional micro analysis. Development of lab on chip on PMMA is carried out for demonstration of drug delivery system. We have demonstrated the micromanipulation of ferrofluid (Nickel Ferrite nano particle dispersed in poly ethylene glycol) using travelling magnetic field. Recently, we have fabricated integrated Bio-MEMS with micropump actuated by magnetohydrodynamics and micro valve operated by Hydrodynamics. Figure T.1.17 shows fabricated device and its assembly on heat sink for its testing [17]. The width of the microchannel is 300 μm and depth is 800 μm. The microvalves are made of PDMS and fitted in corresponding locations. The hydrolysis of water is carried out using 1.5V battery for actuation of PDMS microvalves to bridge a gap of 80 μm between input and output microfluidic channel.

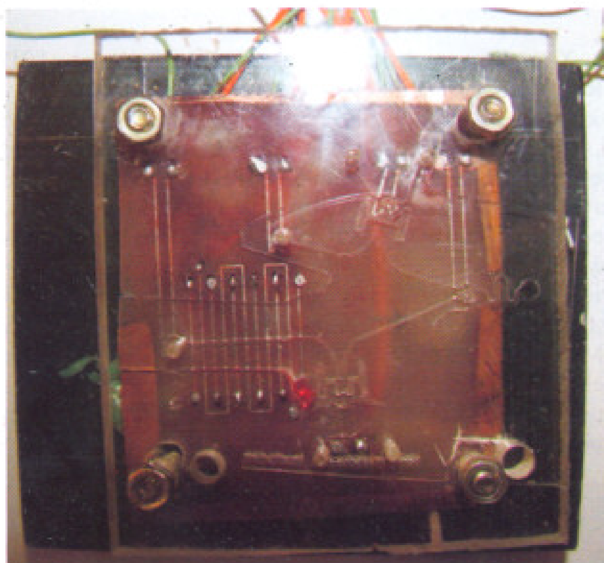

Figure T.1.17: Micropump and microvalves integrated Bio-MEMS for micromanipulation of ferrofluid.

X-ray lithography beamline is operational on Indus-2 for undertaking microfabrication research activities. Beamline is used for fabrication of variety of structures in PMMA/SU-8 for applications in X-ray optics, mechanical engineering and biological science.

References

[1] Ehrfeld W., Muenchmeyer D., 1991 Three-dimensional microfabrication using synchrotron radiation, Nucl Instrum Methods Phys Res A **303** 523.

[2] Kim Guk Bae and Lee Sang Joon, 2007, *Journal of the Korean Physical Society,* **51(4)**, 1256.

[3] Achenbach S., 2004 *Microsystem Technologies,* **10** 493.

[4] Makarova O.V, Tang C.M., Mancini D.D., Moldovan N., Divan R., Ryding D.G., Lee R.H., 2003 *Microsystem Technologies*, **9** 395.

[5] Linke Jian, Bernd Loechel, Heinz-Ulrich Scheunemann, Martin Bednarzik, Yohannes M. Desta, and Jost Goettert, 2003 Proceedings of the International Conference on MEMS, NANO and Smart Systems (ICMENS'03), 0-7695-1947-4/03.

[6] Utsumi Yuichi and Kishimoto Takefumi, 2005 *J. Vac. Sci. Technol.* B **23** 2903.

[7] Khan Malek C., Saile V., Manohara H. and Craft B., 1998, *J. Synchrotron Rad.* **5**, 1095.

[8] Romanato Filippo, Fabrizio Enzo Di, Vaccari Lisa, Altissimo M., Cojoc D., Businaro L., Cabrini Stefano, 2001, *Microelectronic Engineering* **57–58** 101.

[9] Perennes F., Bona F. De, Pantenburg F.J., 2001 *Nuclear Instruments and Methods in Physics Research* A **467–468**, 1274.

[10] Spiller E., Feder R., Topalian J., Catellani E., Romankiw L. and Heritage M., 1976 *Solid State Technol*, **April 1976**, p 62-68

[11] Becker E. W., Ehrfeld W., Munchmeyer D., Betz H., Heuberger A., Pongratz S., Hlsdhsudrt E., Michel H.J. and Siemens V.R, 1982, Naturwissenschaften, **69**, 520-523.

[12] Lodha G.S., Dhamgaye V.P., Modi M. H., Nayak M., Sinha A.K. and Nandedkar R.V., 2007, *Proceedings of SRI 2006*, AIP Volume **879**, 1474.

[13] Dhamgaye V. P. and Lodha G. S., 2004, *RRCAT Internal Report,* **12-2004**.

[14] Mukherjee Shriparna, 2012, *YSRP 2012 thesis* (2012).

[15] Dhamgaye V P and Lodha G S, 2012, DAE SSPS 2011, *AIP Conf Proc*, **1447**, 525.

[16] Sharma Prateek, 2012, *M Tech Thesis.*